Proceedings of the ASME 2010 3rd Joint US-European Fluids Engineering Summer Meeting and 8th International Conference on Nanochannels, Microchannels, and Minichannels
FEDSM-ICNMM2010
August 1-5, 2010, Montreal, Canada

FEDSM-ICNMM2010-30964

THE LS-STAG METHOD FOR VISCOUS INCOMPRESSIBLE FLOWS IN IRREGULAR GEOMETRIES : BASICS OF THE DISCRETIZATION AND APPLICATION TO VISCOELASTIC FLOWS

Olivier Botella
LEMTA, Nancy-University, CNRS
2, avenue de la Forêt de Haye, B.P 160
54504 Vandœuvre-lès-Nancy, France
Email: Olivier.Botella@ensem.inpl-nancy.fr

Yoann Cheny
CERFACS
42 rue Gaspard Coriolis
31057 Toulouse Cedex 01, France
Email: cheny@cerfacs.fr

ABSTRACT

The LS-STAG method is an immersed boundary method for viscous incompressible flows based on the staggered MAC arrangement for Cartesian grids, where the irregular boundary is sharply represented by its level-set function. The level-set function enables us to compute efficiently all relevant geometry parameters of the so-called "cut-cells", i.e. *the cells that are cut by the immersed boundary, reducing thus the bookkeeping associated to the handling of complex geometries. One of the main features of the LS-STAG method is the use of a consistent and unified discretization of the flow equations in both Cartesian and cut-cells, which has been obtained by enforcing the strict conservation of global invariants of the flow such as total mass, momentum and kinetic energy in the whole fluid domain. After a short discussion on the salient features of the LS-STAG method, we will present one of its most recent application : The computation of viscoelastic flows governed by the Oldroyd-B constitutive equation.*

INTRODUCTION

This communication presents an Immersed Boundary (IB) / Finite Volume (FV) method for the computation of incompressible flows in 2D irregular geometries, with an emphasis on viscoelastic flows [1]. Lately, FV methods have drawn a renewed interest for viscoelastic computations, motivated by their inherent low computational costs compared to Finite Element formulations. For Newtonian flows in irregular geometries, IB methods have now reached a high level of maturity (see [2] for a recent review). They rely on cost-effective Cartesian grid methods that alleviate the generation of body fitted meshes and the need of frequent remeshing in the case of problems with moving boundaries. IB methods have found numerous applications in turbulent flows, fluid-structure interaction, biological and biomedical flows, *etc*... To our knowledge, IB methods have not yet been applied to viscoelastic flows.

For modelling the rheology of viscoelastic fluids, the various constitutive equations that have been devised (upper convected Maxwell, Oldroyd-B, Phan-Thien/Tanner, *etc*..., see [3] for a review) have common features : a set of nonlinear hyperbolic transport equations for the elastic part of the stress tensor, that has to be coupled to the incompressible Navier-Stokes equations. The numerical solution of these coupled problems shares the same difficulties, the most severe being the breakdown of the numerical algorithms for highly elastic flows : the so-called *high Weissenberg number problem*, named after the dimensionless parameter We that measures the level of elasticity of the flow [1,3]. To overcome this major numerical challenge, we have identified two issues concerning the spatial and temporal discretizations of the flow equations :

- As for the velocity and pressure coupling for Newtonian flows, the discretization of the velocity and stress has to be compatible for preventing unphysical node-to-node oscillations of the stress variables. For a FV method, this is usually achieved by an adequate staggering of the normal and shear

stress unknowns on the computational grid [4, 5].

- In addition, for preventing the breakdown of the solution caused by the loss of positive-definiteness of the elastic stress tensor during the time integration, a time-stepping strategy that preserves this property at the discrete level must be devised (see [6] and references therein).

This communication presents a progress report on viscoelastic flow computations performed with a well established IB method, the LS-STAG method (see Refs. [7, 8]), that would eventually address all the fundamental numerical issues mentioned above. We recall that for Newtonian flows, the LS-STAG method is based on the staggered MAC method of Verstappen & Veldman [9], where the IB boundary is represented by its level-set function [10]. The discretization in the cut-cells (*i.e.*, the computational cells which are cut by the irregular boundary) is achieved by requiring that the global conservation properties of the Navier-Stokes equations are satisfied at the discrete level, resulting in a stable and accurate method and, thanks to the level-set representation of the IB boundary, at low computational costs. We mention that for constructing this discretization up to the cut-cells, we had to accurately take into account the boundary conditions at the immersed boundaries. To our knowledge, these boundary terms have always been neglected in previous studies, with the exception of the recent work by Jameson [11]. For our viscoelastic computations, we have used the Oldroyd-B model with constant viscosities as the constitutive equation. For building our IB method, we believed that a key ingredient lies in the discretization of the stress equations in the cut-cells, where the viscous effects are prominent. Hence, on the grounds of our discretization of the Newtonian stresses in the cut-cells, we have achieved a fully staggered discretization of the Oldroyd-B equations that ensures a strong coupling of all flow variables, and such that the Cartesian staggered arrangement of Refs. [4, 5] is recovered away from the immersed boundary. The time advancement is based on a fully segregated fractional-step scheme.

In Refs. [7,8], the accuracy and robustness of our method has been assessed on canonical flows at low to moderate Reynolds number : Taylor Couette flow, flows past a circular cylinder, including the case where the cylinder has forced oscillatory rotations. We also have extended the LS-STAG method to flows with moving immersed boundaries without the need for domain remeshing at each time-step, which is one of the most appealing features of IB methods. In the present communication, we will focus on presenting some unpublished results taken from the thesis of Y. Cheny [12] : the computations of a popular benchmark for viscoelastic flows in complex geometries, *i.e.* the four-to-one abrupt planar contraction with rounded re-entrant corners [13–15] for a wide range of Weissenberg numbers.

GOVERNING EQUATIONS

The equations that govern the motion of a viscoelastic Oldroyd-B fluid are [1, 3] :

$$\rho\left(\frac{\partial v}{\partial t}+\nabla\cdot(v\otimes v)\right)=-\nabla p+\eta_s\nabla\cdot(\nabla v)+\nabla\cdot\tau_e, \tag{1a}$$

$$\tau_e+\lambda\overset{\triangledown}{\tau_e}=2\eta_e D, \tag{1b}$$

$$\nabla\cdot v=0, \tag{1c}$$

where ρ is the fluid density, η_s and η_e are respectively the viscosity of the Newtonian solvant and of the polymeric solution that contributes to the fluid elasticity, λ is the elastic characteristic time,= $v=(u,v)$ is the velocity vector in 2D, p is the pressure, and τ_e is the viscoelastic tensor :

$$\tau_e=\begin{pmatrix}\tau_e^{xx} & \tau_e^{xy}\\ \tau_e^{xy} & \tau_e^{yy}\end{pmatrix}. \tag{2}$$

We also denotes $D=\frac{1}{2}\left(\nabla v+\nabla v^T\right)$ the rate-of-strain tensor, and $\overset{\triangledown}{(\cdot)}$ denotes the upper-convected derivative of a tensor :

$$\overset{\triangledown}{A}=\frac{\partial A}{\partial t}+(v\cdot\nabla)A-A\cdot\nabla v^T-\nabla v\cdot A. \tag{3}$$

Thus, in 2D we have 6 scalar variables : in addition to the flow velocity and pressure, we have to consider the extra-stress components τ_e^{xx}, τ_e^{xy} and τ_e^{yy}. When we nondimensionalize System (1) with L and U as the reference length and velocity of the flow, and use $(\eta_s+\eta_e)U/L$ as the reference value for pressure and stress, we obtain a set of 3 nondimensional numbers :

$$\beta=\frac{\eta_s}{\eta_s+\eta_e},\quad \mathrm{We}=\frac{\lambda U}{L},\quad \mathrm{Re}=\frac{\rho UL}{\eta_s+\eta_e}. \tag{4}$$

The first nondimensional number is the viscosity ratio, that measure the amount of solvant in the fluid, and the last two are characteristics of the flow : the Weissenberg number We measures the level of elasticity of the flow, and the Reynolds number Re measures the convective effects. In the limit where there is no solvant in the fluid ($\eta_s=0$), Eqs. (1) recovers the equations for the upper convected Maxwell fluid (UCM), and when there is no elasticity in the flow ($\lambda=0$), Eq. (1b) gives explicitly the extra-stress as

$$\tau_e=2\eta_e D. \tag{5}$$

Thus, we can substitute (5) in the momentum equation (1a) for

recovering the case of the incompressible Navier-Stokes equations for Newtonian fluids :

$$\rho\left(\frac{\partial v}{\partial t}+\nabla\cdot(v\otimes v)\right)=-\nabla p+\eta\nabla\cdot\nabla v, \tag{6a}$$

$$\nabla\cdot v=0, \tag{6b}$$

where $\eta=\eta_s+\eta_e$ denotes the total viscosity.

For solving the Oldroyd-B system (1) by a finite-volume IB method, we have to formulate its integral form on a square domain Ω and use the divergence theorem to recover integrals on the surface Γ of the domain. The integral form of the Navier-Stokes equations (1a),(1c) is well known and will not be repeated here. The integral form of the tensorial equation (1b) for the normal stresses τ_e^{xx}, τ_e^{yy}, and the shear stress τ_e^{xy} is respectively :

$$\lambda\big(\frac{\mathrm{d}}{\mathrm{d}t}\int_\Omega \tau_e^{xx}\,\mathrm{d}V+\int_\Gamma (v\cdot n)\,\tau_e^{xx}\,\mathrm{d}S\big)=S_e^{xx}, \tag{7a}$$

$$\lambda\big(\frac{\mathrm{d}}{\mathrm{d}t}\int_\Omega \tau_e^{yy}\,\mathrm{d}V+\int_\Gamma (v\cdot n)\,\tau_e^{yy}\,\mathrm{d}S\big)=S_e^{yy}, \tag{7b}$$

$$\lambda\big(\frac{\mathrm{d}}{\mathrm{d}t}\int_\Omega \tau_e^{xy}\,\mathrm{d}V+\int_\Gamma (v\cdot n)\,\tau_e^{xy}\,\mathrm{d}S\big)=S_e^{xy}, \tag{7c}$$

where S_e^{xx}, S_e^{yy} and S_e^{xy} are volumic terms which steam from the definition of the upper-convected derivative (3), and that respectively read :

$$S_e^{xx}=\int_\Omega\left[-\tau_e^{xx}+2\lambda\big(\tau_e^{xx}\frac{\partial u}{\partial x}+\tau_e^{xy}\frac{\partial u}{\partial y}\big)+2\eta_e\frac{\partial u}{\partial x}\right]\mathrm{d}V, \tag{8a}$$

$$S_e^{yy}=\int_\Omega\left[-\tau_e^{yy}+2\lambda\big(\tau_e^{yy}\frac{\partial v}{\partial y}+\tau_e^{xy}\frac{\partial v}{\partial x}\big)+2\eta_e\frac{\partial v}{\partial y}\right]\mathrm{d}V, \tag{8b}$$

$$S_e^{xy}=\int_\Omega\left[-\tau_e^{xy}+\lambda\big(\tau_e^{xx}\frac{\partial v}{\partial x}+\tau_e^{yy}\frac{\partial u}{\partial y}\big)+\eta_e\big(\frac{\partial u}{\partial y}+\frac{\partial v}{\partial x}\big)\right]\mathrm{d}V \tag{8c}$$

Suitable initial and boundary conditions have to be specified for the Oldroyd-B system (1) and (7). The usual boundary conditions for Newtonian flows applies for the velocity and pressure, while for the extra-stress τ_e it is important to note that the transport equations for the extra-stress components τ_e are hyperbolic [1,5], and thus only stress values at inflow boundaries have to be specified. In contrast, stress values at solid boundaries are not given and thus have to be computed. At outflow boundaries, Neumann boundary conditions are usually prescribed numerically.

In Refs. [7, 8], we have introduced the LS-STAG method, an IB method that discretizes the Navier-Stokes equations (6) for Newtonian fluids, which is based on the finite volume discretization of Verstappen & Veldman [9] on a staggered non-uniform Cartesian grids. The discretization of the momentum and continuity Eqs. (1a),(1c) is based on common grounds and will be summarized in the next section. The transport equations (7) for the elastic stresses give additional difficulties that form the core of the present paper. Firstly, we will have to define the control volumes for the normal and shear stresses on the LS-STAG mesh, and then we will have to develop novel discretizations the volumic integrals in Eqs. (8), which were absent from the discretization of the Newtonian equations. In contrast, the convective terms in the LHS of Eqs. (7), that involves surface integrals, will be discretized with similar techniques for the convective terms of the momentum equations.

BASICS OF THE LS-STAG METHOD FOR NEWTONIAN FLOWS IN IRREGULAR GEOMETRIES

In this section, we summarize the LS-STAG discretization for the Navier-Stokes equations (6) originally presented in Refs. [7, 8], whose chief property is to preserves the conservation properties (for total mass, momentum and kinetic energy) of the original MAC method when it is applied to complex immersed boundaries. We will give an emphasis to to the definition of the LS-STAG mesh and the discretization of the Newtonian stresses, which will be invaluable for discretizing the Oldroyd-B constitutive equation (7) in the next section.

The LS-STAG Mesh for Immersed Complex Geometries

We consider an irregular solid domain Ω^{ib} which is embedded in a rectangular computational domain Ω, such that $\Omega^{\mathrm{f}}=\Omega\setminus\Omega^{\mathrm{ib}}$ represents the fluid domain where the flow equations are to be discretized. To keep track of the irregular boundary Γ^{ib}, we employ a signed distance function $\phi(x)$ (*i.e.* , the level-set function [10]) such that $\phi(x)$ is negative in the fluid region Ω^{f}, $\phi(x)$ is positive in the solid region Ω^{ib}, and such that the boundary Γ^{ib} corresponds to the zero level-set of this function.

This leads to the extension of the well known MAC mesh (see *e.g.* [9]) that is described in Fig. 1, and that will be subsequently referred to as the *LS-STAG mesh*. In each cut-cell $\Omega_{i,j}$ of size $\Delta x_i\times\Delta y_j$, the immersed boundary is represented by a line segment whose extremities are defined by linear interpolation of the variable $\phi_{i,j}$, which takes the value of the level-set function $\phi(x_i,y_j)$ at the upper right corner of the cell. The faces of the trapezoidal cut-cell $\Omega_{i,j}$ are denoted in Fig. 1 with the usual compass notations :

$$\Gamma_{i,j}=\Gamma^{\mathrm{w}}_{i,j}\cup\Gamma^{\mathrm{e}}_{i,j}\cup\Gamma^{\mathrm{s}}_{i,j}\cup\Gamma^{\mathrm{ib}}_{i,j}, \tag{9}$$

where $\Gamma^{\mathrm{ib}}_{i,j}$ represents the solid north face of the cut-cell. The velocity unknowns are exactly located in the middle of the fluid part of the faces, and the discrete pressure $p_{i,j}$ is positioned inside

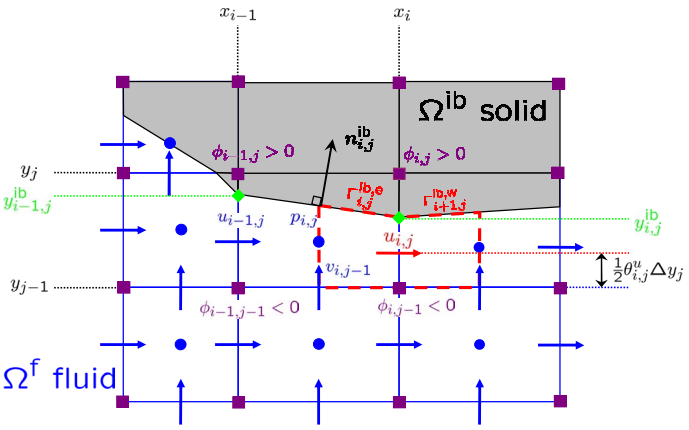

FIGURE 1. STAGGERED ARRANGEMENT OF THE VARIABLES NEAR THE TRAPEZOIDAL CUT-CELL $\Omega_{i,j}$ ON THE LS-STAG MESH. THE CONTROL VOLUME FOR $u_{i,j}$ IS SHOWN IN RED, AND NON-HOMOGENEOUS VELOCITY BOUNDARY CONDITIONS ARE DISCRETIZED AT THE VERTICES (♦) OF THE CUT-CELLS.

the cut-cell : as it is shown in Refs. [7,8] the discrete pressure is piecewise constant in each cut-cell, and thus does not need to be located precisely. The discretization of the elastic tensor that is compatible with this velocity-pressure stencil will be presented in the next section.

In Figure 1, we observe that there are three basic types of cut-cells : *trapezoidal cells* such as $\Omega_{i,j}$ or $\Omega_{i+1,j}$, *triangular cells* (*i.e.* , $\Omega_{i-1,j+1}$) and *pentagonal cells* (*i.e.* , $\Omega_{i-1,j}$). For each basic type of cut-cells, the level-set function will prove to be a very efficient tool for calculating their geometric parameters, such as their volume or the projected areas of their faces. A quantity that will be extensively used for calculating these parameters is the fluid portion of the faces of cell $\Omega_{i,j}$. For example in Figure 1, by using one-dimensional linear interpolation of $\phi(x_i,y)$ in $[y_{j-1},y_j]$, we calculate the length $y^{\rm ib}_{i,j}-y_{j-1}$ of the portion of face $\Gamma^{\rm e}_{i,j}$ that belongs to the fluid domain as :

$$y^{\rm ib}_{i,j}-y_{j-1} = \theta^u_{i,j}\,\Delta y_j, \quad \text{with } \theta^u_{i,j} = \frac{\phi_{i,j-1}}{\phi_{i,j-1}-\phi_{i,j}},$$

since $\phi(x_i,y^{\rm ib}_{i,j})=0$. The scalar quantities $\theta^u_{i,j}$ and $\theta^v_{i,j}$, which take values in $\big[0,1\big]$, will subsequently be called the *cell-face fraction ratios*. They represent the fluid portion of the east and north faces $\Gamma^{\rm e}_{i,j}$ and $\Gamma^{\rm n}_{i,j}$ respectively. They will be extensively used for detecting if the discrete velocities and elastic stress components belong to the fluid domain, and for discretizing the surface and volume integrals in the Oldroyd-B system (7). The cell-face fraction ratios also appear in the analytic expression of the volume $V_{i,j}$ of cell $\Omega_{i,j}$, whose analytic expression is given in [8] for each basic type of cut-cells.

Summary of the LS-STAG Discretization for Newtonian Flows

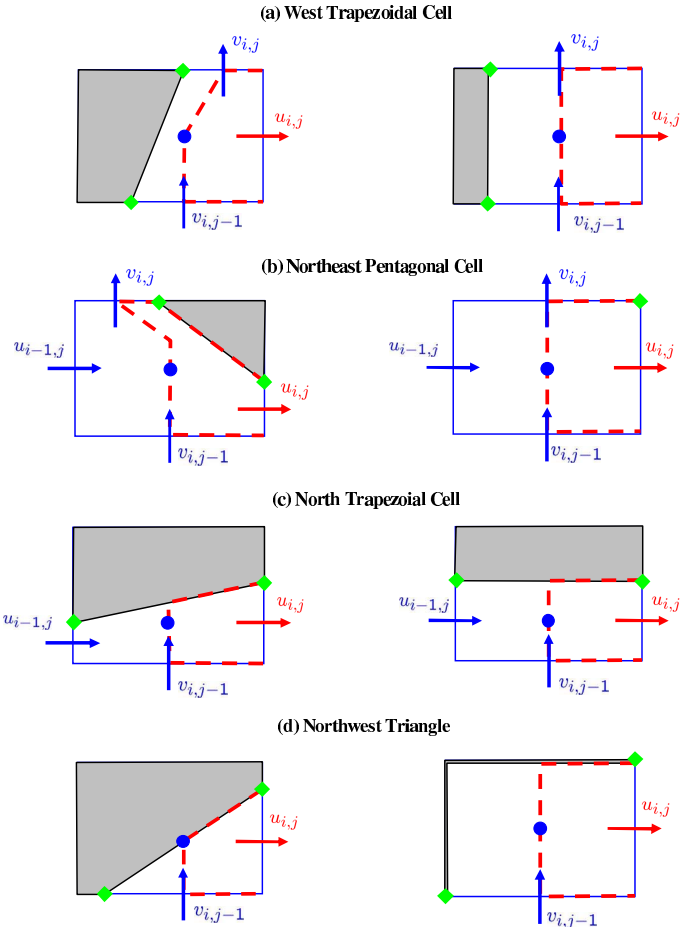

FIGURE 2. FOUR GENERIC TYPES OF CUT-CELLS $\Omega_{i,j}$ (AT LEFT) AND THEIR CORRESPONDING LIMIT CASE (AT RIGHT) FOR CARTESIAN GEOMETRIES. WE HAVE REPRESENTED IN DASHED RED LINE THE HALF-CONTROL VOLUME FOR THE VELOCITY $u_{i,j}$.

In this part, we will give a summary of the LS-STAG discretization of the incompressible Navier-Stokes equations discussed in [7,8]. The discretization of based on the finite volume method, where the continuity equation (6b) is discretized in $\Omega_{i,j}$, and the momentum equation (6a) is discretized in staggered control volumes $\Omega^u_{i,j}$ and $\Omega^v_{i,j}$ for each component of the velocity, whose shapes have to be adapted to each type of cut-cells. For example in Fig. 1, the faces of the control volume $\Omega^u_{i,j}$ for $u_{i,j}$ read :

$$\Gamma^u_{i,j} = \Gamma^{u,\rm w}_{i,j} \cup \Gamma^{u,\rm e}_{i,j} \cup \big(\Gamma^{\rm s,e}_{i,j} \cup \Gamma^{\rm s,w}_{i+1,j}\big) \cup \big(\Gamma^{\rm ib,e}_{i,j} \cup \Gamma^{\rm ib,w}_{i+1,j}\big), \qquad (10)$$

where the solid faces $\Gamma^{\mathrm{ib,e}}_{i,j} \cup \Gamma^{\mathrm{ib,w}}_{i+1,j}$ are formed with two halves of the solid face of the neighboring trapezoidal cut-cells $\Gamma^{\mathrm{ib,e}}_{i,j} \subset \Gamma^{\mathrm{ib}}_{i,j}$ and $\Gamma^{\mathrm{ib,w}}_{i+1,j} \subset \Gamma^{\mathrm{ib}}_{i+1,j}$. For the other type of cut-cells, these control volumes will be constructed from the six halves of generic control volumes that we represent in Figure 2 (left). In this figure, the irregular shape of the staggered control volumes is given for representation purpose only, and their geometric parameters, such as their actual volume or shape of the vertical faces $\Gamma^{u,\mathrm{w}}_{i,j}$ and $\Gamma^{u,\mathrm{e}}_{i,j}$ are never used by the LS-STAG discretization : instead, we will employ arguments based on the strict conservation of total mass, momentum and kinetic energy for discretizing the momentum equations in each of the half-control volume of Figure 2, such that any combination of half CVs yields a consistent discretization with the aforementioned global conservation properties. In the limiting case of Cartesian cells (see Fig. 2 (right)), the LS-STAG method recovers the case of the usual MAC discretization of Harlow & Welch [16] for uniform grids and the method of Verstappen & Veldman [9] for non-uniform grids.

Globally Conservative Discretization on the LS-STAG Mesh

It is now widely recognized (see *e.g.* [9, 11, 17, 18]) that higher stability and accuracy is obtained with numerical methods that conserve the global invariants of the flow such as total mass $\int_{\Omega^{\mathrm{f}}} \nabla \cdot v \, \mathrm{d}V$, total momentum $\mathbf{P}(t) = \rho \int_{\Omega^{\mathrm{f}}} v \, \mathrm{d}V$ and total kinetic energy $\mathrm{E_c}(t) = \frac{1}{2} \int_{\Omega^{\mathrm{f}}} |v|^2 \, \mathrm{d}V$ when viscosity becomes negligible. A numerical method is called "globally conservative" if the discrete equivalent of the transport equations of these quantities are verified. It is well known the original staggered grid method of Harlow & Welch [16] on uniform Cartesian meshes with central differencing of the convective term is "globally conservative". On the other hand, for more general grid systems or higher-order methods the construction of "globally conservative" methods is not a trivial task, and one needs to enforce the conservation properties to the discretization scheme [9, 17, 18]. For example, let us consider the discretization of the Navier-Stokes equations (6) such as its semi-discrete matrix representation reads :

$$\rho \frac{\mathrm{d}}{\mathrm{d}t}(\mathscr{M} U) + \mathscr{C}[\overline{U}]U + \mathscr{G}P - \eta \mathscr{K} U = 0, \tag{11a}$$

$$\mathscr{D} U = 0, \tag{11b}$$

where the diagonal mass matrix $\mathscr{M}$ is built from the volume of the fluid cells, matrix $\mathscr{C}[\overline{U}]$ represents the discretization of the convective fluxes, $\mathscr{G}$ is the discrete pressure gradient, $\mathscr{K}$ represents the Newtonian stresses, and $\mathscr{D}$ is the discrete divergence. For simplicity, we have discarded here the influence of the boundary conditions, but the complete discussion can be found in Ref. [8].

The budget for the discrete energy $\mathrm{E}^h_{\mathrm{c}}(t)$ is obtained from the discrete momentum equation as :

$$\frac{\mathrm{dE}^h_{\mathrm{c}}}{\mathrm{d}t} = -U^{\mathrm{T}} \frac{\mathscr{C}[\overline{U}]^{\mathrm{T}} + \mathscr{C}[\overline{U}]}{2} U - P^{\mathrm{T}} \mathscr{G}^{\mathrm{T}} U - U^{\mathrm{T}} \frac{\eta(\mathscr{K}^{\mathrm{T}} + \mathscr{K})}{2} U, \tag{12}$$

and if we require that this discrete budget mimics the dissipation of energy in the whole fluid domain by the viscous forces, the following conditions have to be enforced on the numerical scheme :

- The discretization of the convective terms should lead to a skew-symmetric matrix :

$$\mathscr{C}[\overline{U}] = -\mathscr{C}[\overline{U}]^{\mathrm{T}}, \tag{13}$$

- the pressure gradient should be dual to the divergence operator :

$$\mathscr{G} = -\mathscr{D}^{\mathrm{T}}, \tag{14}$$

- the viscous matrix $\mathscr{K}^{\mathrm{T}} + \mathscr{K}$ should be positive definite.

As observed in Ref. [9], the skew-symmetry condition (13) amounts to using a centered scheme for the convective terms. In Ref. [8], we have developed a skew-symmetric discretization in the cut-cells of Fig. 2 such as non-homogeneous conditions at the immersed boundary are naturally embedded. Condition (14) and the discrete continuity equation (11b) leads to the following discretization of the pressure gradient on the LS-STAG mesh :

$$\int_{\Gamma^u_{i,j}} p \, e_x \cdot n \, \mathrm{d}S \cong [\mathscr{G}^x P]_{i,j} = \theta^u_{i,j} \Delta y_j \left(p_{i+1,j} - p_{i,j} \right). \tag{15}$$

This formula is valid for any type of fluid cells, and in the particular case of Cartesian fluid cells (such that the cell-face fraction ratios are equal to 1), one recovers the finite-difference gradient of the MAC method.

Discretization of the Newtonian Stresses

Now, we summarize the discretization of the Newtonian viscous stresses, because it has a great importance for the extension of the LS-STAG method to viscoelastic flows. For the $x-$momentum equation, the Newtonian viscous terms written in control volume $\Omega^u_{i,j}$ reads :

$$\int_{\Gamma^u_{i,j}} \nabla u \cdot n \, \mathrm{d}S = \int_{\Gamma^u_{i,j}} \frac{\partial u}{\partial x} e_x \cdot n \, \mathrm{d}S + \int_{\Gamma^u_{i,j}} \frac{\partial u}{\partial y} e_y \cdot n \, \mathrm{d}S. \tag{16}$$

In Refs [7,8], we have proposed an accurate discretization of these terms in the cut-cells such that the simplicity of the 5-point

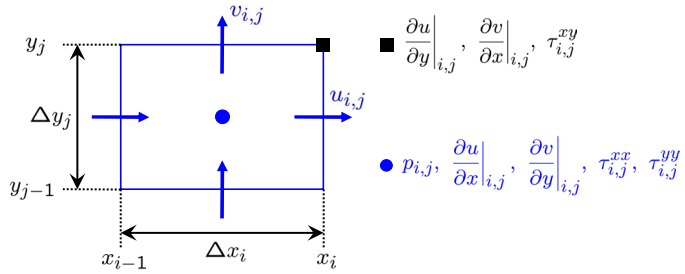

FIGURE 3. STAGGERED ARRANGEMENT OF VELOCITY, PRESSURE AND STRESS IN THE CARTESIAN CELL $\Omega_{i,j}$.

structure of the MAC method be preserved. This has proved to be the most intricate part of the LS-STAG method, and in order to achieve this discretization we had to consider separately the discretization of the shear stresses and the normal stresses. In the MAC mesh of Harlow & Welch [16], the normal stresses are naturally located at the center of a Cartesian cell, while the shear stress is located at its upper right corner (see Fig. 3). Hence on the LS-STAG mesh, it is very natural to locate the shear stresses at the vertices of the cut-cells as shown on Fig 4. Note that for the case of pentagonal cells, $\partial u/\partial y|_{i,j}$ and $\partial v/\partial x|_{i,j}$ are computed at distinct vertices.

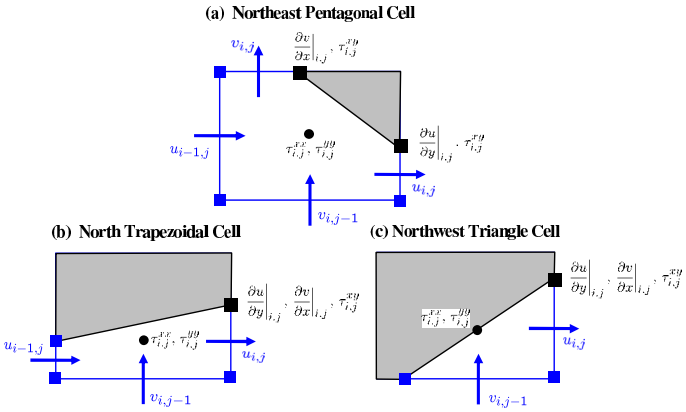

FIGURE 4. LOCATION OF THE NORMAL AND SHEAR STRESSES IN THE 3 GENERIC CUT-CELLS $\Omega_{i,j}$.

The shear stresses are discretized as in the Ghost Fluid Method for elliptic equations [19] : if $\theta^u_{i,j} > 0$ then North cell $\Omega_{i,j+1}$ is a fluid cell and thus we write :

$$\left.\frac{\partial u}{\partial y}\right|_{i,j} = \frac{u_{i,j+1} - u_{i,j}}{\frac{1}{2}\,\theta^u_{i,j}\Delta y_j + \frac{1}{2}\,\theta^u_{i,j+1}\Delta y_{j+1}}, \qquad (17a)$$

where the quotient is computed by differentiating the interpolation polynomial of $u(x_i,\cdot)$ in the vertical direction. If $\theta^u_{i,j} = 0$ then $\Omega_{i,j+1}$ is a solid cell as in Fig. 4, and we use the one-sided quotient :

$$\left.\frac{\partial u}{\partial y}\right|_{i,j} = \frac{u(x_i, y^{\rm ib}_{i,j}) - u_{i,j}}{\frac{1}{2}\,\theta^u_{i,j}\Delta y_j}, \qquad (17b)$$

where $u(x_i, y^{\rm ib}_{i,j})$ is the velocity prescribed at the immersed boundary (see Fig. 1 for notations). In Ref. [8], this discretization is completed by defining the integration areas on each generic cut-cell such that discrete conservation of global momentum holds. An analogous discretization is derived for $\partial v/\partial x|_{i,j}$.

To discretize the normal stresses, we argued in Refs [7, 8] that pressure and normal stress have the same mathematical and physical origin (diagonal part of the stress tensor), and should be discretized with the same formulae. Thus, we discretize the normal stress flux $\int_{\Gamma^u_{i,j}} \frac{\partial u}{\partial x}\, e_x \cdot n\, {\rm d}S$ with an expression similar to the pressure gradient (15), which leads to the following expression :

$$\int_{\Gamma^u_{i,j}} \frac{\partial u}{\partial x}\, e_x \cdot n\, {\rm d}S \cong \theta^u_{i,j}\Delta y_j \left(\left.\frac{\partial u}{\partial x}\right|_{i+1,j} - \left.\frac{\partial u}{\partial x}\right|_{i,j} \right). \qquad (18)$$

The discretization has to be completed with a differential quotient for $\partial u/\partial x|_{i,j}$. In Refs [7, 8], this quotient has been constructed by requiring that Green's theorem be valid at the discrete level in a cut-cell, since it is trivially verified by the *MAC* method in a Cartesian cell. After a straightforward discretization of the integrals and comparison with the continuity equation, one gets :

$$\left.\frac{\partial u}{\partial x}\right|_{i,j} \cong \frac{\theta^u_{i,j}\,u_{i,j} - \theta^u_{i-1,j}\,u_{i-1,j} + (\,\theta^u_{i-1,j} - \theta^u_{i,j}\,)\,u^{\rm ib}_{i,j}}{V_{i,j}/\Delta y_j}, \qquad (19)$$

and an analogous discretization holds for $\partial v/\partial y|_{i,j}$.

Finally, we note that formulas (17) and (19) are valid for any type of cut-cells, with the boundary conditions naturally imbedded. They reduce to the standard finite-difference quotients in the case of a Cartesian fluid cell. Furthermore, we mention that pressure and normal stresses take piecewise constant values in the cut-cells, so they can be located anywhere inside the cell for the sake of interpolation.

THE LS-STAG DISCRETIZATION FOR VISCOELASTIC FLOWS

The first step of the discretization of the Oldroyd-B system (7) is the positioning of the extra-stress unknowns[1] $\tau^{xx}_{i,j}$, $\tau^{xy}_{i,j}$,

[1]Note that for the sake of clarity, the underscript 'e' is dropped in the definition of the discrete components of the extra-stress tensor τ_e.

and $\tau^{yy}_{i,j}$ in the LS-STAG mesh. In effect, the earliest simulations of viscoelastic flows proved that it was extremely difficult to obtain stable numerical solutions when the Weissenberg number We was moderately large, even for steady problems [1]. The loss of convergence of the solution procedure has been subsequently attributed to several causes, and one of the first that has been identified is related to the spurious oscillations of the extra-stress tensor τ_e. It was then acknowledged that the discretization of the extra-stress components τ_e^{xx}, τ_e^{xy} and τ_e^{yy} must be compatible with the velocity and pressure, as much as the pressure and velocity discretizations has to be compatible for Newtonian computations to avoid pressure checkerboarding. Thus for the finite element method, velocity-pressure-stress discretizations that follow a LBB condition have been developed (see the review by Baaijens [20]). For finite volume discretizations, the discrete stress unknowns have to be adequately staggered in the well known MAC mesh for Newtonian flows [16], shown in Fig. 3. The velocity unknowns are set at the middle of the cell faces and the pressure at the center of the cell. *i.e.* the normal stresses $\tau^{xx}_{i,j}$ and $\tau^{yy}_{i,j}$ are at the center of the cell $\Omega_{i,j}$ and the shear stress $\tau^{xy}_{i,j}$ at its upper right corner. In this way, when the level of elasticity becomes negligible ($\lambda = 0$), the discretization of the Oldroyd-B system (1) recovers the case of Newtonian fluids, see Eqs. (5) and (6).

This staggered arrangement was first introduced by Darwish & Whiteman [4], and later used by [5,21,22]. In the cut-cells, the discretization of the Newtonian stresses presented above entices us to position the extra-stresses as shown in Fig. 4. Note that, in this figure, we conveniently locate $\tau^{xx}_{i,j}$ and $\tau^{yy}_{i,j}$ at the centroid of the cut-cells but, as stated in the previous section, the normal stresses take constant values in the cut-cells. For the case of pentagonal cells (see Fig. 4(a)), where the Newtonian shear stresses $\partial u/\partial y|_{i,j}$ and $\partial v/\partial x|_{i,j}$ are calculated at different vertices of the immersed boundary, we consider that $\tau^{xy}_{i,j}$ takes the same value at both vertices. Finally, we mention that this discretization has much in common with the finite element method for viscoelastic flows of Saramito [23], which uses a mixed Raviart-Thomas element where pressure and normal stresses are discretized with piecewise constant polynomials with a degree of freedom at the element centroid, while the shear stress is discretized with a linear continuous polynomial with degrees of freedom at the element vertices.

In the context of a finite-volume method, the use of this staggered arrangement introduces a different control volume for each transport equation of the Oldroyd-B system (7). Thus, the new difficulty encountered compared to the Newtonian method of Refs. [7, 8] lies in the quadrature of the volumic terms in the RHS (8) of the transport equations, that have to be adapted to the case of normal and shear stresses. To develop these quadrature, we will use conservation properties of the transport equations in the spirit of the LS-STAG method for Newtonian flows. The starting point is the discretization of the normal stress equations, and then it will be adapted to the shear stress equations such that global conservation holds for all transport equations.

For discretizing the transport equation (7a) for τ_e^{xx}, it is natural to consider $\Omega_{i,j}$ as the control volume. We first start the discretization of the volumic terms in the RHS of (8a), *i.e.* :

$$\begin{aligned} S^{xx}_{i,j} = &- \underbrace{\int_{\Omega_{i,j}} \tau_e^{xx}\,\mathrm{d}V}_{①} + 2\lambda \underbrace{\int_{\Omega_{i,j}} \tau_e^{xx}\frac{\partial u}{\partial x}\,\mathrm{d}V}_{②} \\ &+ 2\lambda \underbrace{\int_{\Omega_{i,j}} \tau_e^{xy}\frac{\partial u}{\partial y}\,\mathrm{d}V}_{③} + 2\eta_e \underbrace{\int_{\Omega_{i,j}} \frac{\partial u}{\partial x}\,\mathrm{d}V}_{④}. \end{aligned} \tag{20}$$

For the underlined terms ①, ② and ④, the quadrature is straightforward since the integrands are considered constant in each cut-cell : for example midpoint rule applied to Term ② gives simply :

$$\int_{\Omega_{i,j}} \tau_e^{xx}\frac{\partial u}{\partial x}\,\mathrm{d}V \simeq \tau^{xx}_{i,j}\left.\frac{\partial u}{\partial x}\right|_{i,j} V_{i,j}, \tag{21}$$

where $V_{i,j}$ is the area of the cell and $\partial u/\partial x|_{i,j}$ is given by Eq. (19). Analogous quadrature holds for terms ①, ④ and the time-derivative term $\frac{\mathrm{d}}{\mathrm{d}t}\int_{\Omega_{i,j}} \tau_e^{xx}\,\mathrm{d}V$.

The discretization of Term ③ is totally different since both terms of the integrand are defined at the vertices of the fluid cells, and the number of these vertices depends on the type of the cells. Hence, we will discretize this term in two consecutive steps. First, midpoint quadrature yields :

$$\int_{\Omega_{i,j}} \tau_e^{xy}\frac{\partial u}{\partial y}\,\mathrm{d}V \cong \left[\tau_e^{xy}\frac{\partial u}{\partial y}\right]^{\mathrm{c}}_{i,j} V_{i,j}, \tag{22}$$

where $\left[\tau_e^{xy}\frac{\partial u}{\partial y}\right]^{\mathrm{c}}_{i,j}$ refers to the mean value of the integrand in cut-cell $\Omega_{i,j}$. This mean value is calculated differently depending on the type of the cell. For the case of the Cartesian cell of Fig. 3, pentagonal cut-cell of Fig. 4(a), and trapezoidal cut-cell of Fig. 4(b), we define this mean value as :

$$\begin{aligned} \left[\tau_e^{xy}\frac{\partial u}{\partial y}\right]^{\mathrm{c}}_{i,j} = &\frac{1}{4}\tau^{xy}_{i,j}\left.\frac{\partial u}{\partial y}\right|_{i,j} + \frac{1}{4}\tau^{xy}_{i-1,j}\left.\frac{\partial u}{\partial y}\right|_{i-1,j} \\ &+ \frac{1}{4}\tau^{xy}_{i-1,j-1}\left.\frac{\partial u}{\partial y}\right|_{i-1,j-1} + \frac{1}{4}\tau^{xy}_{i,j-1}\left.\frac{\partial u}{\partial y}\right|_{i,j-1}, \end{aligned} \tag{23a}$$

and for the triangular cell of Fig. 4(c) we define the 3-point mean value :

$$\left[\tau_{\mathrm{e}}^{xy}\frac{\partial u}{\partial y}\right]^{\mathrm{c}}_{i,j} = \frac{1}{3}\tau^{xy}_{i,j}\left.\frac{\partial u}{\partial y}\right|_{i,j} + \frac{1}{3}\tau^{xy}_{i-1,j-1}\left.\frac{\partial u}{\partial y}\right|_{i-1,j-1} + \frac{1}{3}\tau^{xy}_{i,j-1}\left.\frac{\partial u}{\partial y}\right|_{i,j-1}. \tag{23b}$$

For both definitions of the mean value, the Newtonian shear stress $\partial u/\partial y|_{i,j}$ is calculated as (17a) or (17b) according to its position on the LS-STAG mesh, and thus the boundary conditions are naturally implemented in these terms.

The discretization of the convective term $\int_{\Gamma_{i,j}}(v\cdot n)\,\tau_{\mathrm{e}}^{xx}\,\mathrm{d}S$ in the LHS of Eq. (8a) follows the lines of the Newtonian discretization in Refs [7, 8], except that we shall not use skew-symmetric (*i.e.*, central) discretization for an hyperbolic equation such as Eq. (7a). Instead, the first-order upwind discretization will be employed in this work (see Ref. [12] for details). Upwind interpolation has the merits to give a monotone discretization of the convective terms, even if its accuracy is limited to first-order and is very diffusive when the flow direction is not aligned with the mesh. But we mention that higher-order monotone discretization can be easily adapted to the LS-STAG discretization, and is left for future work.

In summary, the LS-STAG discretization of the transport equation (7a) for τ_{e}^{xx} can be written in matrix form as the semi-discrete equation :

$$\lambda\left(\mathscr{M}_{\mathrm{e}}^{xx}\frac{\mathrm{d}T_{\mathrm{e}}^{xx}}{\mathrm{d}t} + \mathscr{C}_{\mathrm{e}}^{xx}[\overline{U}]T_{\mathrm{e}}^{xx}\right) = -\mathscr{M}_{\mathrm{e}}^{xx}T_{\mathrm{e}}^{xx} + S_{\mathrm{e}}^{xx}[T,U], \tag{24}$$

where T_{e}^{xx} is the vector containing the extra-stress unknowns $\tau_{i,j}^{xx}$, $\mathscr{M}_{\mathrm{e}}^{xx}$ is the diagonal mass matrix whose entries correspond to the cell areas $V_{i,j}$, the matrix $\mathscr{C}_{\mathrm{e}}^{xx}[\overline{U}]$ corresponds to the discretization of the convective terms, $\mathscr{M}_{\mathrm{e}}^{xx}T_{\mathrm{e}}^{xx}$ corresponds to the discretization of Term ① in the RHS (20) and $S_{\mathrm{e}}^{xx}[T,U]$ is the discretization of the remaining terms. An equation analogous to (24) is obtained for the transport equation of τ_{e}^{yy}, with $\mathscr{M}_{\mathrm{e}}^{yy} = \mathscr{M}_{\mathrm{e}}^{xx}$ since both discretizations are performed on the same control volume.

If we want to state the conservation properties of the semi-discrete transport equation (24) in the fashion of our previous works [7, 8], we would say that this equation is conservatives in the sense that the mass matrix $\mathscr{M}_{\mathrm{e}}^{xx}$ yields a consistent quadrature in the whole fluid domain Ω_{f} when it is summed on all fluid cells (Cartesian an cut-cells), *i.e.* :

$$\int_{\Omega^{\mathrm{f}}}\tau_{\mathrm{e}}^{xx}\,\mathrm{d}V \cong \sum_{\text{Fluid cells }\Omega_{i,j}} V_{i,j}\,\tau_{i,j}^{xx} = \mathbb{1}^{\mathrm{T}}\mathscr{M}_{\mathrm{e}}^{xx}\,T_{\mathrm{e}}^{xx}, \tag{25}$$

where $\mathbb{1}$ is the constant vector. In particular, if the normal stress is constant ($T^{xx} = \mathbb{1}$) then one recovers the area of the whole fluid domain :

$$\mathrm{Area}(\Omega^{\mathrm{f}}) \cong \sum_{\text{Fluid cells }\Omega_{i,j}} V_{i,j} = \mathbb{1}^{\mathrm{T}}\mathscr{M}_{\mathrm{e}}^{xx}\mathbb{1}. \tag{26}$$

Analogously, thanks to the property of local conservation of the fluxes at fluid faces, the convective discretization verifies the following conservation properties :

$$\mathbb{1}^{\mathrm{T}}\mathscr{C}_{\mathrm{e}}^{xx}[\overline{U}] = 0. \tag{27}$$

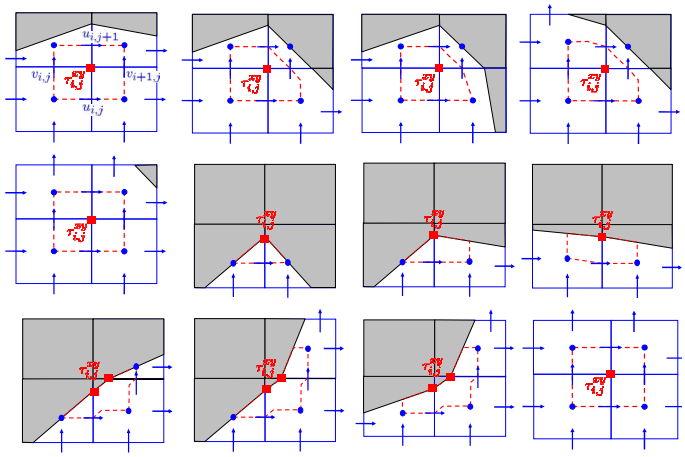

FIGURE 5. GENERIC TYPES OF CONTROL VOLUMES $\widetilde{\Omega}_{i,j}$ FOR THE SHEAR STRESS $\tau_{i,j}^{xy}$ IN THE LS-STAG MESH.

The semi-discretization of the transport equation (7c) for τ_{e}^{xy} is now performed in the staggered control volumes $\widetilde{\Omega}_{i,j}$ that are depicted in Fig. 5. The main difficulty for discretizing the shear stress equation lies in the precise definition of $\widetilde{\Omega}_{i,j}$ from the neighboring cells, the calculation of its geometric parameters, and the fact that building a discretization for each of the special cases of Fig. 5 can be a demanding task. Instead, we will use an effective strategy that has been defined in [7, 8] for the momentum equations : the discretization will be performed independently for each quarter of cell, such that any combination of four quarters of cell yields a consistent discretization that follows a conservation property analogous to (25). We refer to Ref. [12] for the complete description of the discretization.

The time-integration of the semi-discrete Oldroyd-B system (11), (24) is performed with the extension of our well established time-stepping algorithm of Ref. [8] (ie, an AB/BDF2 semi-implicit fractional-step scheme) to viscoelastic problems, except that we have tentatively implemented a first-order version only. This fractional-step algorithm is defined by the following three steps : Firstly, a prediction of the velocity at time

$t_{n+1} = (n+1)\Delta t$, denoted $\widetilde{U}$, is computed by means of the following Euler scheme :

$$\rho \mathscr{M} \frac{\widetilde{U} - U^n}{\Delta t} + \mathscr{C}[U^n]U^n - \mathscr{D}^{\mathrm{T}} P^n - \eta_{\mathrm{s}} \mathscr{K} \widetilde{U} - \mathscr{D}_{\mathrm{e}} T_{\mathrm{e}}^n = 0, \quad (28)$$

where $\mathscr{D}_{\mathrm{e}} T_{\mathrm{e}}$ corresponds to the extra-stress contribution in Eq. (1a). Then, the provisional velocity is corrected to get a solenoidal velocity and the corresponding pressure field :

$$\rho \mathscr{M} \frac{U^{n+1} - \widetilde{U}}{\Delta t} - \mathscr{D}^{\mathrm{T}} \left(P^{n+1} - P^n \right) = 0, \quad (29a)$$

$$\mathscr{D} U^{n+1} = 0. \quad (29b)$$

Now that U^{n+1} is determined, we can employ it to time-advance the extra-stress equations :

$$\lambda \mathscr{M}_{\mathrm{e}} \frac{T_{\mathrm{e}}^{n+1} - T_{\mathrm{e}}^n}{\Delta t} + \mathscr{C}_{\mathrm{e}}[U^{n+1}] T_{\mathrm{e}}^n = -\mathscr{M}_{\mathrm{e}} T_{\mathrm{e}}^{n+1} + S_{\mathrm{e}}[T_{\mathrm{e}}^n, U^{n+1}], \quad (30)$$

where the vector T_{e}^n contains both normal and shear stresses unknowns.

NUMERICAL APPLICATION : FLOW OF VISCOELASTIC OLDROYD-B IN A PLANAR CONTRACTION

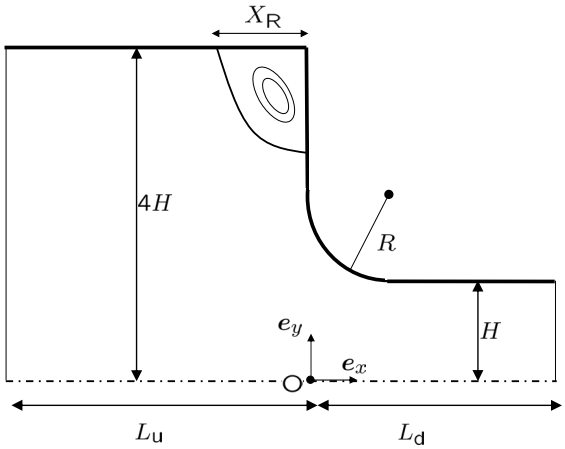

FIGURE 6. SKETCH OF THE 4:1 PLANAR CONTRACTION.

In this section, we have selected some results from the unpublished thesis of Y. Cheny [12]. These computations concern a popular benchmark for viscoelastic flows in complex geometries : the creeping flow of an Oldroyd-B fluid in a 4:1 planar contraction with rounded re-entrant corners [13–15], see Fig. 6. The characteristic length and velocity of the flow are set equal to the height H and the bulk velocity in the downstream half-channel. A steady Poiseuille profile is imposed at the inlet $x = -16H$, an outflow condition is imposed at $x = 16H$, and a slip condition is imposed at the symmetry plane $y = 0$. The results reported here have been obtained on the mesh shown in Fig. 7, for which grid-independent results were reached. Fig. 8 shows that the LS-STAG method predicts accurately the decrease of the intensity of the salient vortex when the level of elasticity increases. As observed in Fig. 9, the stress contours are free from any spurious oscillations thanks to the fully staggered arrangement of the flow variables. In particular, we have checked that the stress boundary layer along the downstream wall is well resolved at all elasticity levels, in contrary to the body-conformal results of Ref. [15]. Table 1 reports some quantitative results of the flow for increasing values of the elasticity level. They are compared to benchmark results obtained with body-conformal methods [14,15] and, where they are available, a good agreement is met with the literature.

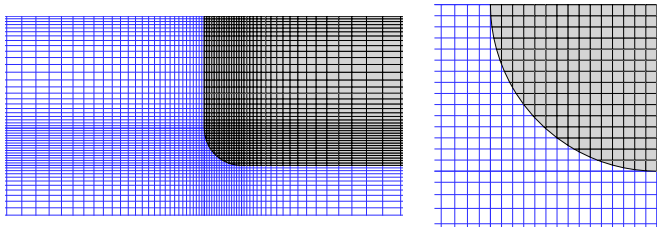

FIGURE 7. CLOSE-UPS OF THE CARTESIAN 96×50 GRID NEAR THE CONTRACTION AND THE RE-ENTRANT CORNER.

CONCLUSION

In this communication, we have presented the salient features of the LS-STAG discretization of viscoelastic flow equations. In particular, we have achieved in the cut-cells a compatible velocity-pressure-stress discretization that prevents node-to-node oscillations of the stress variables. It is also very interesting to note that when the fluid domain is Cartesian, the LS-STAG discretization actually computes the shear stress at solid walls and at salient or reentrant corners, in contrast to previous staggered grid methods that use *ad hoc* interpolations at solid boundaries [4] or at salient corners [21].

A further improvement of the LS-STAG method for viscoelastic flows concerns the development of a time-stepping algorithm that would preserve the positive-definiteness of the elastic stress tensor, in order to mitigate the breakdown of the numerical algorithms when the flow becomes highly elastic [1, 6].

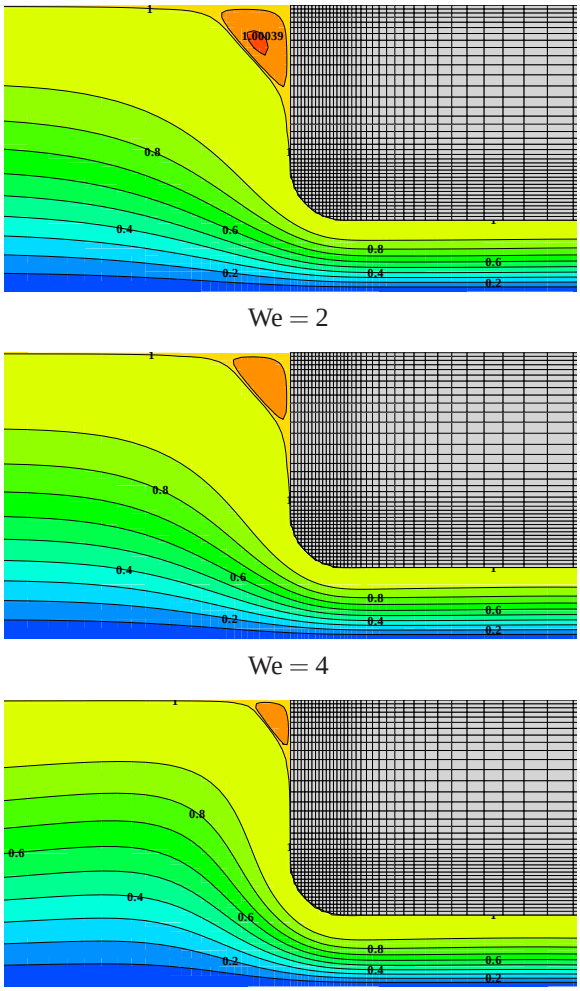

FIGURE 8. STREAMLINES CONTOURS FOR INCREASING VALUES OF THE WEISSENBERG NUMBER We.

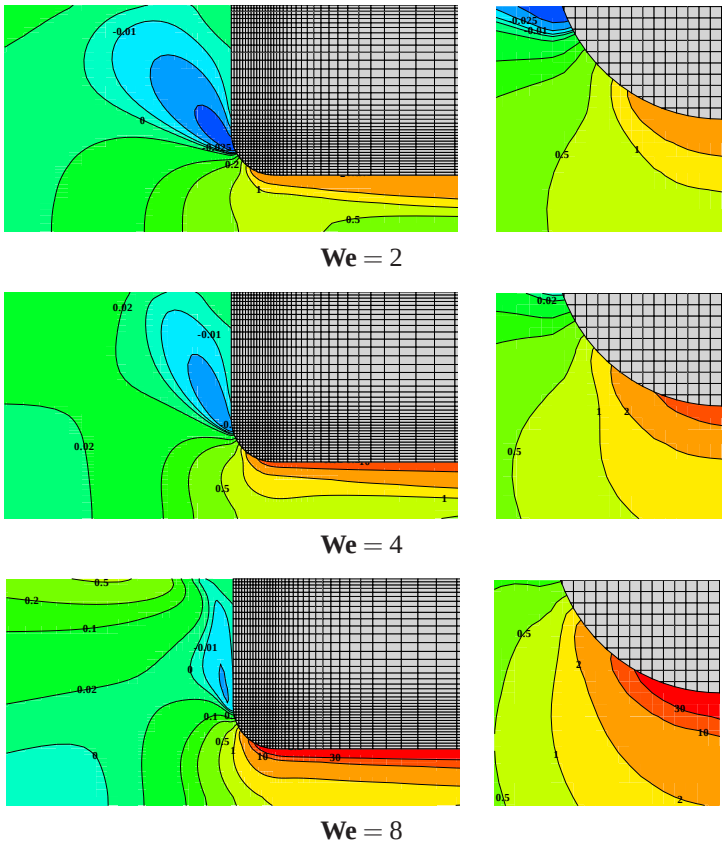

FIGURE 9. ISOVALUES OF THE NORMAL STRESS τ^{xx}. AT RIGHT : CLOSE-UP OF THE FLOW NEAR THE RE-ENTRANT CORNER.

REFERENCES

[1] Owens, R. G., and Phillips, T. N., 2002. *Computational Rheology*. Imperial College Press, London.

[2] Mittal, R., and Iaccarino, G., 2005. "Immersed boundary methods". *Annu. Rev. Fluid Mech.,* **37, *239-261***.

[3] Bird, R. B., Armstrong, R. C., and Hassager, O., 1987. *Dynamics of Polymeric liquids*. Wiley-Interscience, New-York.

[4] Darwish, M., and Whiteman, J., 1992. "Numerical modeling of viscoelastic liquids using a finite-volume method". *J. Non-Newtonian Fluid Mech.,* **45, *311-337***.

[5] Gerritsma, M., 1996. *Time dependant numerical simulations of a viscoelastic fluid on a staggered grid*. PhD thesis, University of Groningen, The Netherlands.

[6] Hao, J., Pan, T.-W., Glowinski, R., and Joseph, D., 2009. "A fictitious domain/distributed Lagrange multiplier method for the particulate flow of Oldroyd-B fluids: A positive definiteness preserving approach". *Journal of Non-Newtonian Fluid Mechanics,* **156, *95 - 111***.

[7] Cheny, Y., and Botella, O., 2009. "An immersed boundary/level-set method for incompressible viscous flows in complex geometries with good conservation properties". *Europ. J. Comput. Mech.,* **18, *561-587***.

[8] Cheny, Y., and Botella, O., 2010. "The LS-STAG method : A new immersed boundary / level-set method for the computation of incompressible viscous flows in complex moving geometries with good conservation properties". *J. Comput. Phys.,* **229, *1043-1076***.

[9] Verstappen, R. W. C. P., and Veldman, A. E. P., 2003. "Symmetry-preserving discretization of turbulent flow". *J. Comput. Phys.,* **187, *343-368***.

[10] Osher, S., and Fedkiw, R. P., 2003. *Level Set Methods and Dynamic Implicit Surfaces*. Springer, New-York.

[11] Jameson, A., 2008. "The construction of discretely conservative finite volume schemes that also globally conserve energy or entropy". *Journal of Scientific Computing,* **34,**

TABLE 1. PROPERTIES OF THE SALIENT CORNER VORTEX AND COUETTE COEFFICIENT C FOR INCREASING VALUES OF THE WEISSENBERG NUMBER We.

		X_R	$\Delta\Psi \times 10^{-3}$	C
We=1	LS-STAG	1.195	0.500	-1.128
	Ref. [15]	–	0.452	-0.69
We=2	LS-STAG	1.095	0.368	-1.469
	Ref. [15]	–	0.342	-1.72
	Ref. [14]	–	0.48	-0.69
We=3	LS-STAG	1.007	0.297	-2.718
	Ref. [15]	–	0.225	-2.67
We=4	LS-STAG	0.923	0.249	-2.843
	Ref. [15]	–	0.225	-3.54
	Ref. [14]	–	0.33	-1.44
We=6	LS-STAG	0.764	0.207	-3.154
	Ref. [14]	–	0.26	-2.27
We=8	LS-STAG	0.602	0.236	-2.834

152-187.

[12] Cheny, Y., 2009. *La Méthode LS-STAG : une nouvelle Approche de type Frontière Immergée/Level-Set pour la Simulation d'Écoulements Visqueux Incompressibles en Géométries Complexes. Application aux Fluides Newtoniens et Viscoélastiques*. Thèse de Doctorat, Université Henri Poincaré - Nancy Université.

[13] Keiller, R. A., 1993. "Entry-flow calculations for the Oldroyd-B and FENE equations". *J. Non-Newtonian Fluid Mech.,* **46, *143-178***.

[14] Matallah, H., Townsend, P., and Webster, M. F., 1998. "Recovery and stress-splitting schemes for viscoelastic flows". *J. Non-Newtonian Fluid Mech.,* **75, *139-166***.

[15] Aboubacar, M., Matallah, H., and Webster, M., 2002. "Highly elastic solutions for Oldroyd-B and Phan-Thien/Tanner fluids with a finite volume/element method: Planar contraction flows". *J. Non-Newtonian Fluid Mech.,* **103, *65-103***.

[16] Harlow, F. H., and Welch, J. E., 1965. "Numerical calculation of time-dependent viscous incompressible flow of fluid with free surfaces". *Phys. Fluids,* **8, *2181-2189***.

[17] Arakawa, A., 1966. "Computational design for long-term numerical integration of the equations of fluid motion : two-dimensional incompressible flow, part I". *J. Comput. Phys.,* **1, *119-143***.

[18] Morinishi, Y., Lund, T. S., Vasilyev, O. V., and Moin, P., 1998. "Fully conservative higher order finite difference schemes for incompressible flow". *J. Comput. Phys.,* **143, *90-124***.

[19] Gibou, F., Fedkiw, R. P., Cheng, L.-T., and Kang, M., 2002. "A second-order-accurate symmetric discretization of the Poisson equation on irregular domains". *J. Comput. Phys.*, **176, *205-227***.

[20] Baaijens, F. P., 1998. "Mixed finite element methods for viscoelastic flow analysis: a review". *Journal of Non-Newtonian Fluid Mechanics,* **79,*361 - 385***.

[21] Phillips, T., and Williams, A., 1999. "Viscoelastic flow through a planar contraction using a semi-Lagrangian finite volume method". *J. Non-Newtonian Fluid Mech.,* **87, *215-246***.

[22] Mompean, G., and Deville, M., 1997. "Unsteady finite volume simulation of Oldroyd-B fluid through a three-dimensional planar contraction". *J. Non-Newtonian Fluid Mech.,* **872, *253-279***.

[23] Saramito, P., 1994. "Numerical simulation of viscoelastic fluid flows using incompressible finite element method and a θ-method". *Mathematical Modelling and Numerical Analysis,* **28, *1-35***.